New Journal of Physics
The open-access journal for physics

The northern site of the Pierre Auger Observatory

Johannes Blümer[1] **and the Pierre Auger Collaboration**[2]
Karlsruhe Institute of Technology (KIT)[3], PO Box 3640, D-76021 Karlsruhe, Germany
E-mail: johannes.bluemer@kit.edu

New Journal of Physics **12** (2010) 035001 (21pp)
Received 18 August 2009
Published 9 March 2010
Online at http://www.njp.org/
doi:10.1088/1367-2630/12/3/035001

Abstract. The Pierre Auger Observatory is an international facility dedicated to the full-sky study of the highest-energy cosmic rays. The southern site of the Auger Observatory was completed in June 2008. Data collected since January 2004 have yielded important information on the energy spectrum, the primary particle composition, the fluxes of photons and neutrinos and on the anisotropic distribution of the arrival directions of the most energetic particles. On this basis, the scientific motivation for the northern Auger Observatory site in Colorado, USA, is discussed. The overall layout, the key components and the expected performance of this 20 000 km^2 hybrid observatory comprised of an array of 4400 surface detectors and 39 fluorescence telescopes are described.

[1] Author to whom any correspondence should be addressed.
[2] The most recent author list is available at http://www.auger.org/admin/Collaborators/author_list_alphabetical.html.
[3] KIT is the cooperation of Universität Karlsruhe (TH) and Forschungszentrum Karlsruhe GmbH.

Contents

1. Introduction

Cosmic rays are messengers from space that cover energies from less than a GeV to more than 10^{20} eV. The history of cosmic rays begins with their discovery by Victor Hess in 1912 [1]. Extensive air showers were recorded and recognized by Pierre Auger in 1938 [2]. A steepening of the energy spectrum around 10^{15} eV was found by Kulikov and Khristiansen in 1958, the so-called knee [3]. John Linsley reported the first event with energy greater than 10^{20} eV in 1963 [4], and Greisen, Zatsepin and Kuzmin predicted in 1966 that there would be 'an end to the cosmic ray spectrum' due to the interaction of protons with the omni-present cosmic microwave background photons above a threshold energy of 6×10^{19} eV. This is the so-called Greisen–Zatsepin–Kuzmin (GZK) effect [5]. A flattening of the spectrum, the ankle, was established in the early 1990s by pioneering measurements using the Volcano Ranch, SUGAR, Haverah Park, Yakutsk, AGASA and Fly's Eye instruments; see [6] for a detailed account of these foundations of cosmic ray research. The KASCADE group demonstrated in 2002 that the knee was caused by a decrease of the flux of light particles, while the heavier primaries showed no change of the spectral index [7]. The anisotropic distribution of arrival directions at energies above $\approx 6 \times 10^{19}$ eV was measured for the first time by the Pierre Auger Observatory in 2007 [8]. The HiRes and Auger collaborations published energy spectra in 2008, which are compatible with the GZK feature predicted 40 years ago [9, 10].

A recent review and references to further information can be found in [11]; this also contains the collection of published measurements of the cosmic ray flux $J(E)$ over a wide range of energies shown in figure 1. In this representation, $J(E) \times E^{2.5}$ is plotted to better identify spectral features.

A coherent description of the particle physics and astrophysics of the extremely rich phenomena of cosmic rays is emerging; however, it is still incomplete and many important questions cannot be answered yet. In this paper, we focus on progress in understanding the most

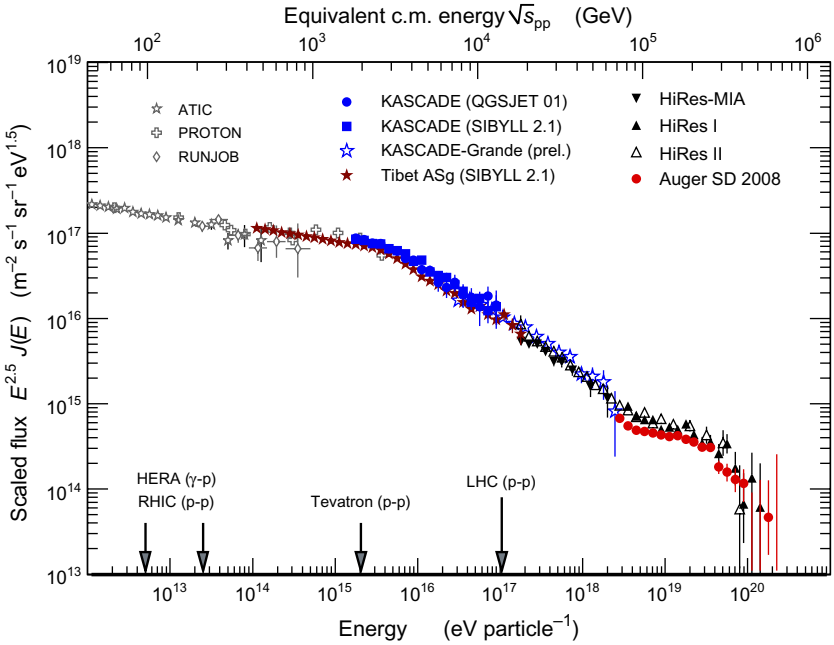

Figure 1. All-particle cosmic-ray energy spectrum as obtained by various direct measurements above the atmosphere and by air shower detectors. See [11] for references and further details.

energetic particles from space, i.e. with energies above 10^{18} eV $\equiv$ 1 EeV. They confront us with some of the most interesting and challenging questions in science today. Where do they come from? What kind of particles are they? How can they be accelerated to such high energies? What can we learn about cosmic objects, large-scale structure and magnetic fields? What can we learn about particle interactions at 300 TeV in the centre-of-mass system?

The answers to these questions may have far-reaching implications. Theoretical scenarios for the acceleration include supermassive black holes, explosive gamma-ray bursts (GRBs), shocks in clusters and filaments throughout the universe, the birth of neutron stars or magnetars at the coalescence of binary systems, and shocks in magnetized radio lobes. Exotic explanations like the decay of relics from the early universe or of super-heavy dark matter particles are now less favoured and are tightly bound by new limits on the photon flux at the highest energies. The propagation from extragalactic sources to Earth may enable investigations of cosmic magnetic fields and of the distribution of matter in our cosmic vicinity. Particle interactions in showers can be studied using the detailed measurements made possible by fluorescence telescopes. Hence, the measurement of ultra-high energy (UHE) cosmic rays offers unique opportunities to study physics and astrophysics under the most extreme conditions.

The prospects for making significant progress are very good at the beginning of the decade, 2010–2020 (see e.g. [12]). In this paper, we first summarize the current results obtained with the southern site of the Pierre Auger Observatory (*Auger South* for short) within the global context. From these observations, we derive the updated scientific motivation for the long-standing plan to achieve full-sky coverage with the Pierre Auger Observatory, and we present the technical layout of the northern site (*Auger North*) in south-east Colorado, USA.

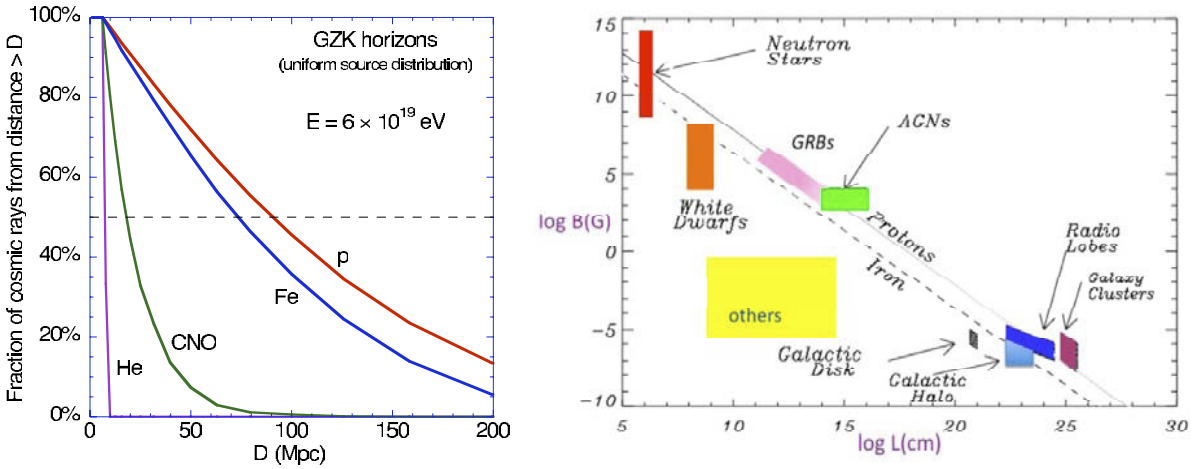

(a) Attenuation of different nuclei (b) Hillas plot

Figure 2. (a) Iron nuclei have attenuation lengths similar to protons, while nuclei of intermediate mass are destroyed already over short propagation distances D. (b) The Hillas plot shows the capabilities of astrophysical objects with size L and magnetic field B to accelerate protons (solid line) or iron nuclei (dashed line) to 100 EeV.

2. Current status

The propagation of protons and heavier nuclei through the cosmic background radiation fields has received much attention recently. A significant result of advanced calculations is that the effective path lengths for protons and iron are quite similar, while nuclei of intermediate mass are broken up due to photo-disintegration. The fraction of remaining protons and heavier nuclei of 60 EeV over distances up to 200 Mpc is shown in figure 2(a); the graph is taken from [12] and based on a comprehensive study [13]. For future analyses, the change of composition during propagation and the effect of magnetic fields will have to be taken into account. The short energy loss lengths indicate that cosmic rays of energy above 100 EeV should come from sources within a 100–200 Mpc sphere. Astrophysical sources within our galaxy are disfavoured. As cosmic rays of energy greater than 10 EeV are no longer confined by galactic magnetic fields, it is natural to assume that they are produced by extra-galactic sources. The list of the very few viable candidate sources for such energies includes active galactic nuclei (AGN), radio lobes of FR II galaxies and GRBs. The so-called Hillas plot in figure 2(b) shows the typical magnetic field B of potential cosmic accelerators versus their size L. In the simplest approximation, the maximum energy of accelerated particles of charge Z can be estimated by requiring that their gyroradius be less than L, i.e. $E_{\max} < ZBL$.

In alternative, non-acceleration scenarios UHE cosmic rays are produced in decays of super-heavy objects such as super-heavy dark matter or topological defects. All of these models postulate new particle physics and predict typically high gamma-ray fluxes at UHE. They are now disfavoured except for the highest energies due to already stringent limits on the flux of photons as shown in figure 6.

The Pierre Auger Collaboration comprises more than 350 scientists in 18 countries. The southern site in Mendoza, Argentina, consists of 1600 water-Cherenkov detectors spread

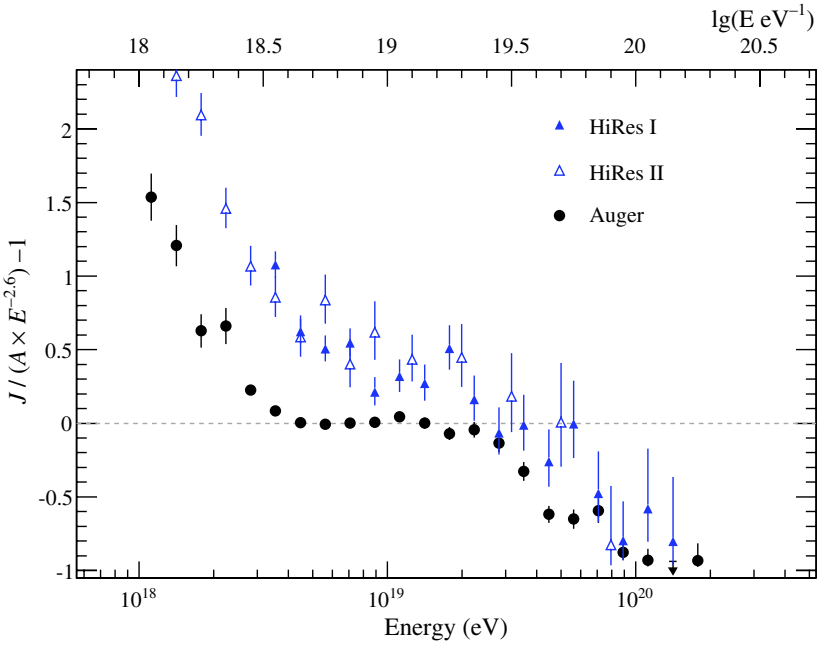

Figure 3. The Auger energy spectrum is compared to a spectrum with an index of 2.6; these data represent the 2009 hybrid measurement, in which SD and FD observations are combined to cover a larger energy range. The optical measurement by the HiRes collaboration is also shown.

over 3000 km^2 on a triangular grid with 1500 m spacing. The surface detector (SD) array is overlooked by 24 electronic telescopes arranged in six stations at the perimeter of the SD. These fluorescence detectors (FDs) record images of the faint, ultraviolet (UV) fluorescence light excited by the air showers. The Auger Observatory is a hybrid system integrating the SD and FD components. The SD operates with 100% duty cycle and the effective aperture can easily be determined; the FD yields a calorimetric optical shower detection and can be calibrated with very little dependence on shower models. The details of the longitudinal shower development are directly observable on $\approx 10\%$ of the events, in particular, the depth of the shower maximum, $X_{\max}$.

The acceptance for zenith angles up to 60° yields a nominal aperture of 7000 km^2 sr. Eventually, showers with larger zenith angles will be reconstructed routinely and added to the data set.

The properties and performance of the Auger instruments have been published in [14]–[16]. The physics results mentioned here are described in more detail in the presentations to the International Cosmic Ray Conferences (ICRC) conferences since 2005; most of them have now been published, as referenced. The reader is also referred to [17] from a previous Focus Issue of this journal.

Auger South has been collecting physics data since January 2004. The results are summarized here very briefly to underline the motivation for the concept of the northern site.

Figure 3 gives a detailed view of the most recent measurement of the energy spectrum obtained with the Auger Observatory [19]. The corresponding exposure is 12 790 km^2 sr yr. The ankle at 3–4 EeV and the GZK-like flux suppression starting at 20–30 EeV are clearly visible.

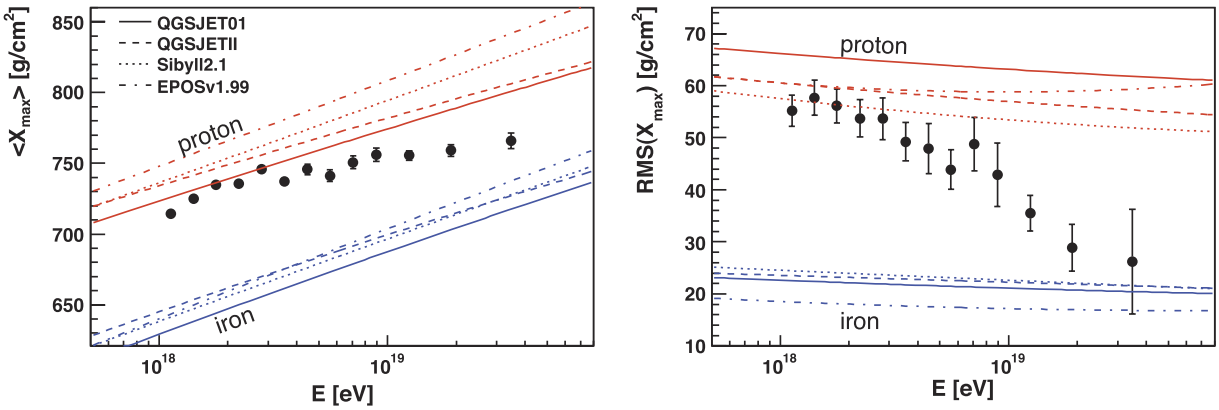

Figure 4. The depth of the shower maximum and the RMS fluctuations as a function of energy show a trend towards lower values; the instrumental resolution has been unfolded. The graphs suggest a heavier composition at the highest energies, see text.

It is worth noting that the exact numerical values of such energies are less important at this time due to possible future shifts of the energy scale by ≈20% by all experimental observations concerned.

The best estimator for the mass of a primary particle initiating an extensive air shower is the depth of shower maximum, which is directly observable with the FD. We show in figure 4 the 2009 result of the dependence of $X_{\max}$ on energy, the so-called elongation rate [20]. There is a trend in the mean $X_{\max}$ towards higher interaction altitudes in the atmosphere, while the fluctuations of $X_{\max}$ decrease to the value expected for heavy nuclei. It is worthwhile noting that such a narrow RMS can only be measured due to the excellent resolution of the FD telescopes (about 20 g cm^{-2}). Implicitly, the graphs give an interpretation in terms of cosmic ray composition, the data points move towards the iron line above $\geqslant$ 10 EeV. It should be noted that increased cross sections and modified multiplicities in the particle production at the first interactions yield similar consequences; see Ulrich *et al* in this NJP issue for a discussion of these aspects [21]. The evolution of $X_{\max}$ with energy is currently under investigation.

At energies above 60 EeV, the arrival directions of cosmic rays become anisotropic. In particular, a correlation between the distributions of arrival directions and of AGN listed in the Veron–Cetty and Veron (VCV) catalogue has been found. In figure 5(a), we show an equatorial projection of the arrival directions of the 27 most energetic particles (energy >55 EeV, adapted from [8] published in 2007). Since then, the data reconstruction and calibration procedures of the Auger Observatory have been updated and the exposure has been nearly doubled. In figure 5(b), we show the degree of correlation (p_{data}) with objects in the VCV catalogue as a function of the total number of time-ordered events. The data collected during the first period from 1 January 2004 through 26 May 2006 was scanned to establish the parameters that maximize the correlation (not shown). Period II refers to the interval from 27 May 2006 through 31 August 2007 and Period III includes data collected after [8], from 1 September 2007 to 31 March 2009. The current estimate of the correlation signal is 0.38 ± 0.07, more than two standard deviations from the value expected from an isotropic distribution of events. More data are needed to accurately constrain this parameter. The anisotropy of the arrival directions as such is a robust feature e.g. in the two-point autocorrelation function. In figure 5(c), we

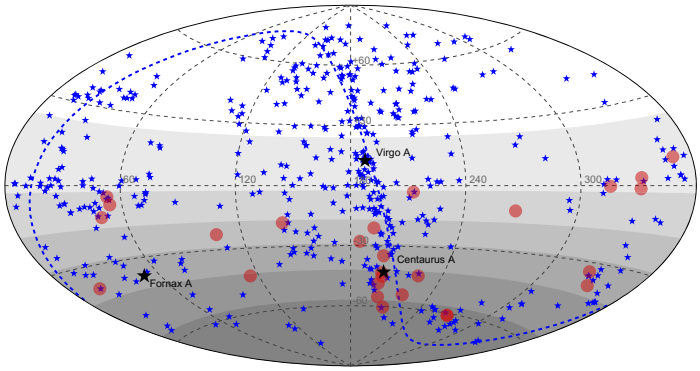

(a) Auger sky map, 2007

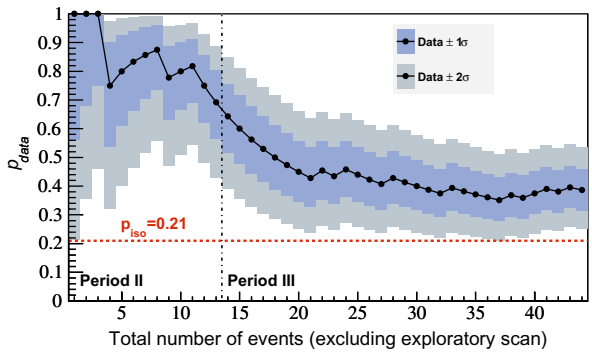

(b) Evolution of correlation signal, 2009

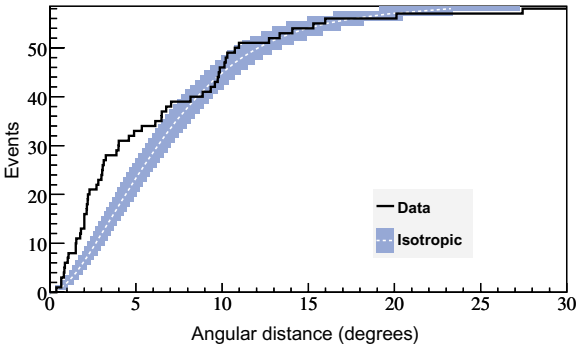

(c) Angular distance from AGN, 2009

Figure 5. (a) Equatorial projection of the celestial sphere: the red circles of radius 3.1° are centred at the arrival directions of the 27 most energetic cosmic rays detected by the Pierre Auger Observatory up to 31 August 2007; nearby AGN from the VCV catalogue are plotted as blue stars. The grey shading indicates areas of equal exposure. (b) The most likely value of the correlation strength is plotted with black dots as a function of time. The 1σ and 2σ uncertainties in the observed value are shaded. The horizontal dashed line shows the isotropic value $p_{\rm iso} = 0.21$. (c) Cumulative number of events as a function of angular distance from the closest AGN in the VCV catalogue for 58 events above 55 EeV using data up to 31 March 2009. The 68% confidence intervals for the isotropic expectation is shaded blue.

show the cumulative number of events as a function of angular distance from the closest AGN in the VCV catalogue for these events. There is also an excess of events from the supergalactic plane and from Centaurus A, a much-debated potential source of extragalactic cosmic rays. Previous analyses have shown no evidence for a significant excess of cosmic rays in the EeV range from the galactic centre, for clustering on different angular scales at the highest energies and for correlations with BL Lac objects. The reader is referred to [22, 23] for more details.

The so-called top-down, non-acceleration models for the origin of the most energetic particles have been invented, which postulate the decay or annihilation of relic topological

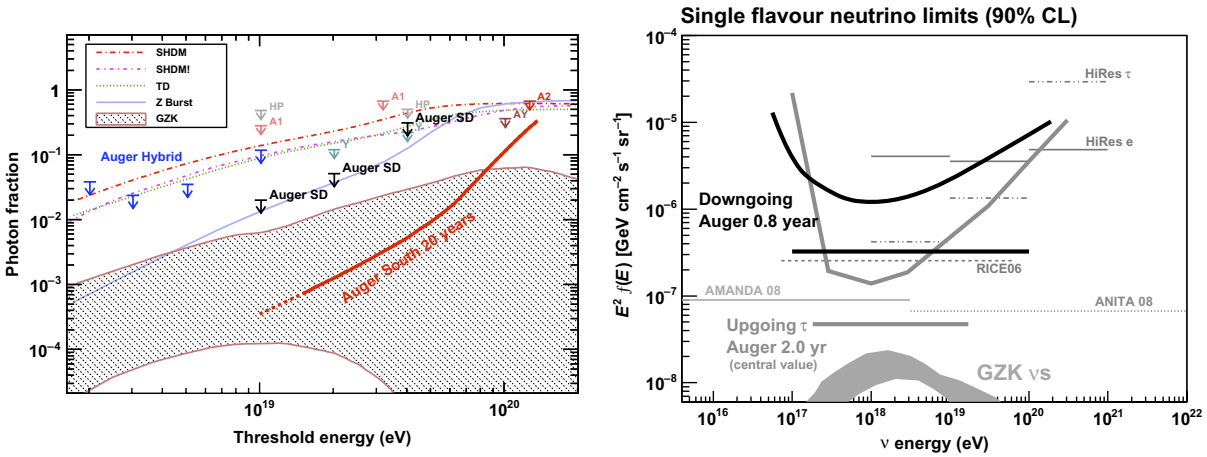

(a) Photon limits, 2009 (b) Neutrino limits, 2009

Figure 6. (a) Upper limits on the cosmic ray photon fraction. The labels *Auger SD* and *Auger Hybrid* refer to results from the Auger SD array and from the recent FD data providing a low-energy extension. The thick red line indicates the sensitivity of Auger South after 20 years of operation. The other lines indicate predictions from top-down models and the shaded region shows the expected GZK photon fraction. The labels shown here are explained in [25]. (b) Differential and integrated upper limits (90% C.L.) for a diffuse flux of down-going neutrinos in the period 1 November 2007–28 February 2009 and up-going neutrinos (1 January 2004–28 February 2009). Limits from other experiments [27] are also plotted. A theoretical flux for GZK neutrinos from [28] is shown.

defects, super-heavy Dark Matter particles or Z bosons. Such models predict relatively high photon fluxes, but depend also on assumptions on the photon propagation in radio background and inter-galactic magnetic fields (see [24]). The typical range of energy loss lengths usually adopted for photons are 7–15 Mpc at 10 EeV and 5–30 Mpc at 100 EeV. Data from the Auger Observatory restrict the photon fraction to less than 2% above 10 EeV at the 95% confidence level. Figure 6 shows this situation together with current limits on the three-flavour neutrino flux, which is less than 5×10^{-8} GeV cm^{-2} s^{-1} sr^{-1} corresponding to neutrino energies between 0.2 and 20 EeV. These limits have been published in [20, 25, 26].

The southern site of the Auger Observatory with its 1.5 km triangular spacing and an area of 3000 km^2 will be able to measure accurately the spectrum and composition from below 1 EeV to about 100 EeV in the next anticipated 10–15 years of operation. To further improve these capabilities, instrumental enhancements are currently being installed close to the Coihueco FD station. These include underground muon detectors, additional water Cherenkov detectors, high-elevation fluorescence telescopes for a larger field-of-view and radio antennae to record the geo-synchrotron emission of air showers.

The operation of Auger South, the performance of detector systems and the instrumental enhancements for the future, including Auger North, are described in [29].

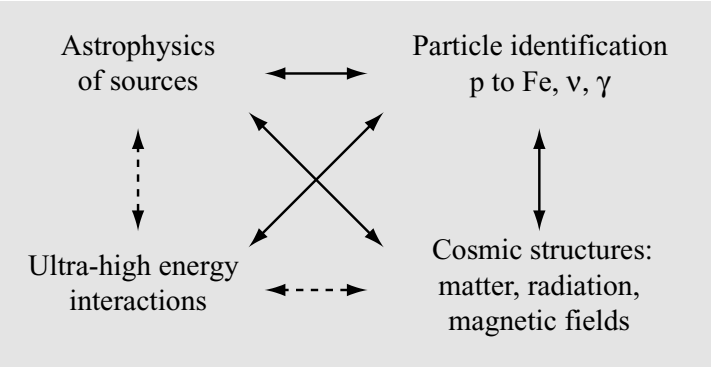

Figure 7. Ultra-high energy cosmic rays are tools to study four science topics in astroparticle physics that are strongly or very strongly interrelated, as indicated by the arrows.

3. Motivation and physics potential for Auger North

The recent results mentioned above represent a significant scientific breakthrough in the field. The energy spectrum shows a feature at the highest energies which is consistent with the GZK effect predicted 40 years ago. Moreover, it is now evident that there is a detectable flux of particles from extragalactic sources within the GZK sphere. The inhomogeneous distribution of matter in the local universe imprints its anisotropy on the arrival directions of cosmic rays above 60 EeV. The challenge is to collect enough such arrival directions to identify the individual sources and study their properties. However, the effect of sources reaching their maximum energy cannot yet be distinguished from the GZK effect. Only above 60 EeV is there anisotropy to exploit for identifying the sources. Moreover, at that energy the primary particles must be primarily protons or heavy nuclei. Light and intermediate nuclei photodisintegrate too rapidly. The southern site of the Auger Observatory in Argentina collects only about 25 of the crucial trans-GZK events per year, with fewer than two per year (on average) that have their longitudinal profiles measured by the air FD. This low rate is not sufficient to achieve the objectives of identifying the sources and studying the pure beam interactions.

The scientific challenge is to follow up the open questions in at least four topics in astroparticle physics: (i) in the astrophysics of the extragalactic sources of the most energetic particles, (ii) in the understanding of the nature of particles that can be nuclei, photons or neutrinos, (iii) in the determination of cosmic structures in a wide sense, including matter, radiation fields and magnetic fields, and (iv) in studying UHE interactions in air showers at energies that are not accessible with man-made accelerators. All of these issues are interrelated, as shown in figure 7. In more detail, the goals include

- Determining the class of astrophysical sources within the GZK sphere that produces trans-GZK particles.
- Identifying some individual discrete sources and measuring the energy spectra of the brightest. Using multi-messenger information to determine the acceleration mechanism and the physical conditions that enable it.
- Determining the primary particle type(s) of trans-GZK cosmic rays. Calculating a reliable spectrum for the diffuse flux of UHE neutrinos and a reliable spectrum for the diffuse

flux of UHE photons resulting from interactions of those trans-GZK particles with all background radiation fields.

- Detecting UHE neutrinos and measuring the diffuse neutrino flux at EeV energies. Also searching for neutrino emission from the identified trans-GZK cosmic ray sources.
- Detecting UHE photons, measuring the diffuse photon spectrum and searching for photons emitted by the identified trans-GZK cosmic ray sources.
- Using magnetic deflections of the charged trans-GZK particles to study the galactic and intergalactic magnetic fields.
- Determining the composition of UHE cosmic rays.
- Determining properties of hadronic interactions in the centre-of-mass energy range 250–450 TeV if the cosmic rays are protons. Measuring the cross section as a function of energy and constraining the inelasticity and multiplicity.
- If the primary trans-GZK cosmic rays are heavy nuclei, air shower studies will probe properties of a quark-gluon plasma produced in nucleus–nucleus collisions at centre-of-mass energies 33–60 TeV per nucleon.

The large aperture of Auger North will make it possible to detect sources in all parts of the sky and to measure energy spectra of individual sources. This is the path to understand the acceleration of high energy cosmic rays, the environments of the accelerators and the interactions and deflections of the particles on their way to Earth.

The northern site of the Auger Observatory is designed with a strong focus on achieving higher statistics at energies above 60 EeV, where the GZK effect makes it possible to study nearby sources without the isotropic background from the rest of the far universe. The goals are ambitious: the angular scale of the AGN correlation and the GZK-like spectral feature suggest that trans-GZK particles are protons. In contrast, the penetration depth of showers and the small fluctuations in this parameter point to heavier primaries. The distinction between the *proton scenario* and *iron scenario* will only be possible with the two complementary sites: the Auger Observatory will study hadronic interactions with good statistics over a wide range of energies up to centre-of-mass energies greater than 300 TeV. As an example, the large aperture of Auger North with fluorescence telescopes will enable the extension of the $X_{\max}$ measurements shown in figure 4 up to 100 EeV with good precision. In addition, the magnetic deflection of cosmic rays en route from known source positions will provide a powerful probe of galactic and intergalactic magnetic fields. Finally, the Auger Observatory should detect cosmogenic neutrinos and photons as well as astrophysical neutrinos and photons coming straight from cosmic ray accelerators in the EeV range. The photon sensitivity shown in figure 6(a) will scale approximately with exposure; the neutrino sensitivity of Auger North will be roughly the same as for Auger South due to the higher energy threshold.

There is also great potential for discoveries that cannot be anticipated. New astrophysical windows invariably yield unexpected phenomena. Auger North will have a large enough aperture to open a new window to the cosmos using trans-GZK cosmic rays. Independent of their astrophysical messages, moreover, these messengers themselves may yield new insights into fundamental interactions at energies that cannot be attained in collider experiments. There may also be surprises in high-exposure views of the universe using UHE photons and UHE neutrinos.

Multi-messenger astronomy, combining detection of charged cosmic rays, of electromagnetic radiation from radio waves to highest-energy gamma rays, of neutrinos and—ultimately—of gravitational waves will be at the forefront of astrophysics and astroparticle physics

during the coming decade and will provide the tools to identify cosmic accelerators and their mechanisms. We plan to strengthen our interactions with the collaborations working in those fields.

4. The site and configuration of Auger North

Auger North will reuse the well-proven detector components developed for Auger South. The focus on the most energetic particles in the universe is reflected in the layout as a relatively sparse array with the largest conceivable instrumented area. The SD array will be covered by fluorescence telescopes as much as possible to ensure the best possible particle identification and for studying particle physics at the energy frontier.

The site, chosen in 2005, is located in the South-East corner of the State of Colorado (USA). The average altitude is about 1300 m above sea level (m a.s.l.). The landscape is almost flat, gently rolling and open; it offers an exceptionally large area of more than 8000 miles^2 (20 000 km^2), possibly further extendable into the state of Kansas. An important feature is the system of county roads, which are spaced on a rectangular one-mile grid covering a large fraction of the anticipated deployment area.

The SD array will consist of 4000 SDs deployed on a rectangular pattern on every second corner of the one-mile grid, alternating in adjacent lines such that a nominal detector spacing of 2.3 km ($\sqrt{2} \times 1$ mile) is obtained. The total area is 8000 miles^2 or 20 000 km^2. Simulations suggest that this configuration reaches 50% efficiency at 8–10 EeV and 100% efficiency at 80 EeV, see section 6. Approximately 10% of the area will be in-filled with 400 additional SDs that will be placed on empty positions of the base grid; this denser part of the array will achieve full efficiency already at 10 EeV for a subset of the events.

Almost full coverage of the SD system will be achieved with 39 fluorescence telescopes arranged in five stations, anticipating a usable viewing distance of 40 km.

A peer-to-peer data communication rather than a direct transmission from SD stations to centralized receivers will be used to guarantee a reliable data flow for SDs located in shallow valleys. Numerous connection points into the existing fibre network across the site are available.

The main features of the two sites are compared in table 1. Technically, the construction of Auger North could begin in 2011.

Construction and operation of a giant detector array relies on the support and cooperation of the people who live within the site and in neighbouring communities. The Auger Observatory is an attraction that ignites curiosity about the large-scale structure of the universe and also the elementary constituents of matter and energy. Our visitor centre in Malargüe has been very popular with about 6000 visitors annually since 2000, and a corresponding outreach effort is underway in Colorado. The Auger Observatory is a highlight of public education and outreach efforts in all member countries.

5. Components of Auger North

Research and development works to improve performance and reduce cost started some time ago and activity on the northern site in south-east Colorado is growing. Changes concerning the water Cherenkov stations include the use of only one PMT tube, insulation against water freezing and new local electronics. The fluorescence telescopes will incorporate new electronics as well, and further improvements already being tested with the new HEAT telescopes

Table 1. Comparison of the Pierre Auger Observatory sites. The energy ranges for the efficiency refer to iron and proton primaries, respectively.

	Auger South	Auger North
Location	35° S, 69° W	38° N, 102°30′ W
Altitude (m a.s.l.)	1300–1500	1300
Area (km^2)	3000	20000
Number of SDs	1600	4000
(infill)		(400)
SD spacing	1500 m	2300 m
(infill)		(1600 m)
Photomultiplier (PMT) sensors per SD	3	1
Communications network	SD-tower radio	Peer-to-peer
SD array 50% efficient at	0.7–1 EeV	8–10 EeV
SD array 100% efficient at	3 EeV	80 EeV
FD stations	4	5
FD telescopes	24 (4 × 6)	39 (2 × 12 + 2 × 6 + 3)
Begin construction	1999	2011
End construction	2008	2016

mentioned at the end of section 2. As a result, Auger North will have seven times the collecting power of Auger South, while the cost factor is only 2.3.

5.1. The SD

The water Cherenkov detectors for Auger North will have a footprint of 10 m^2. The height of 1.5 m will be filled to 1.2 m with ultra-pure water. A model tank is displayed in figure 9. Tanks will be manufactured from high-density polyethylene by the roto-moulding technique and equipped with a thick layer of thermal insulation due to the cold winters in Colorado, featuring temperatures down to −35 °C. The water will be contained in a flexible, laminated liner conforming approximately to the inner tank surface. The innermost lamination consists of Tyvek(R). In this way, the Cherenkov light is diffusively reflected inside the water volume and viewed by the PMT through an optical window. The liner also prevents contamination of the water, which is obtained by distillation, reverse osmosis and UV sterilization to achieve a resistivity above 10 MΩ cm and less than 100 ppb organic carbons. The local communities of Lamar and La Junta have agreed to provide the water.

A single solar panel of 55 Wp will be coupled to a 12 V battery of approximately 100 Ah capacity. All components are common within the solar power industry.

A local data acquisition system performs the following tasks: data acquisition, second level trigger, calibration, slow control and communication with the Central Data Acquisition System (CDAS). The operating system will be a flavour of Real-Time Linux, which will be stored in flash EPROM, and can be downloaded from CDAS.

Only one central PMT will be used, instead of the three used in Auger South. The main specifications are: linearity better than 5% up to 80 mA and a single photoelectron resolution (peak to valley ratio) better than 1.2. The dynamic range of 15 bits in Auger South will

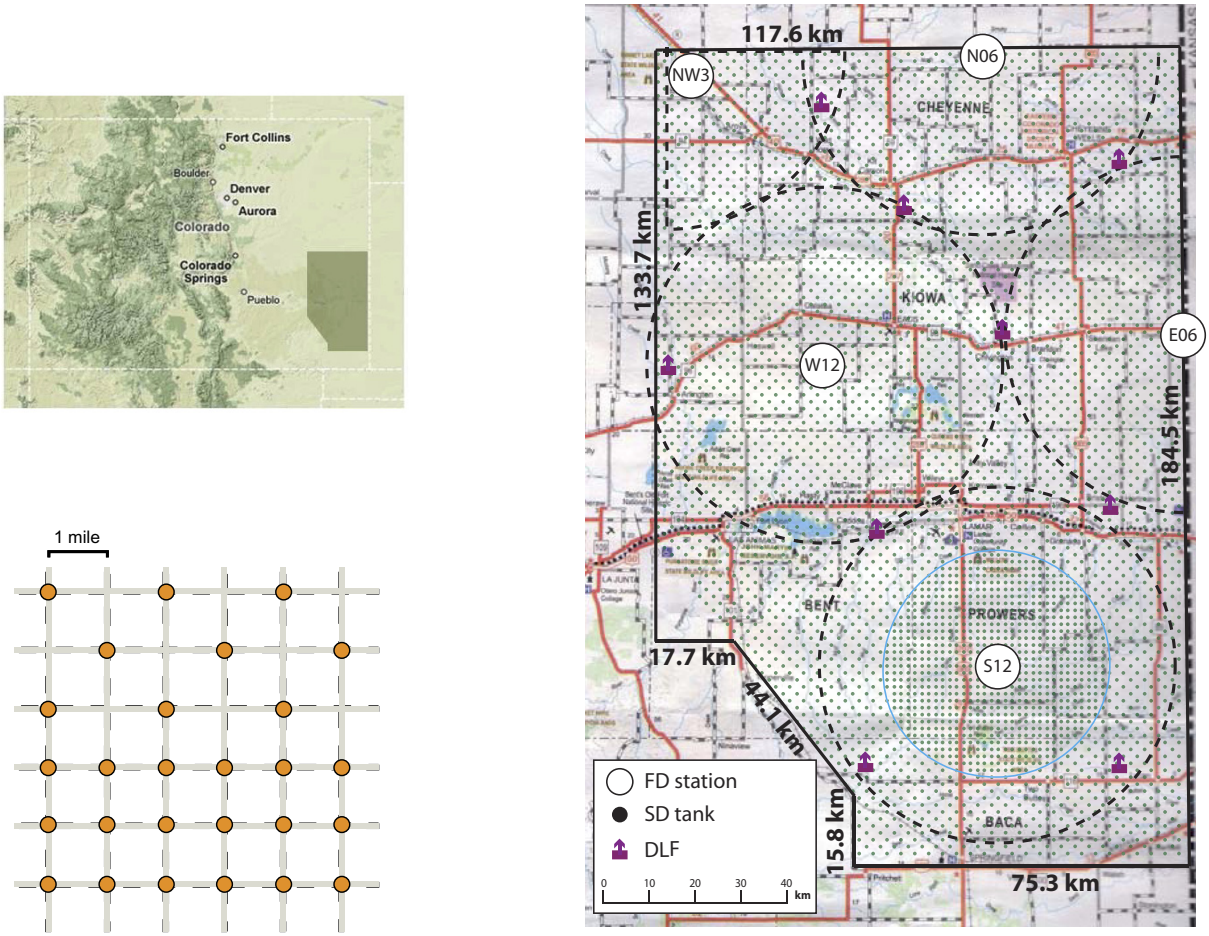

(a) Site location and SD grids

(b) Site map of Auger North

Figure 8. (a) Location of the northern Auger site in Colorado, USA. The lower panel illustrates the deployment options of SD stations with spacings of 1.6 km (1 mile) and with 2.3 km. (b) Site map with each dot representing one water Cherenkov tank. The proposed positions of the fluorescence buildings are also shown together with the DLF. The red area around station S12 contains the in-fill array with a narrower spacing of 1 mile.

be increased to 22 bits by coupling the readout to intermediate dynodes. The digitization is performed with commercial 10-bit ADCs with 100 MHz sampling rate. A simple threshold plus a digital time-over-threshold requirement provides an efficient first-level trigger. A second-level trigger reduces the initial trigger rate from 100 to 20 Hz. Only the time of the second-level trigger and a rough energy estimation are sent to the central system every second. The events are stored locally until they get sent to the central system upon request of a third-level trigger. A GPS clock is used to obtain uniform time calibration across the array to better than 10 ns.

Calibration data will be sent together with event data. The detector calibration is derived from background muons that produce a distinct muon charge spectrum shown in figure 9(b). The peak position corresponding to nearly vertical muons defines the Vertical Equivalent Muon (VEM) unit, which is then used in all SD signal measurements.

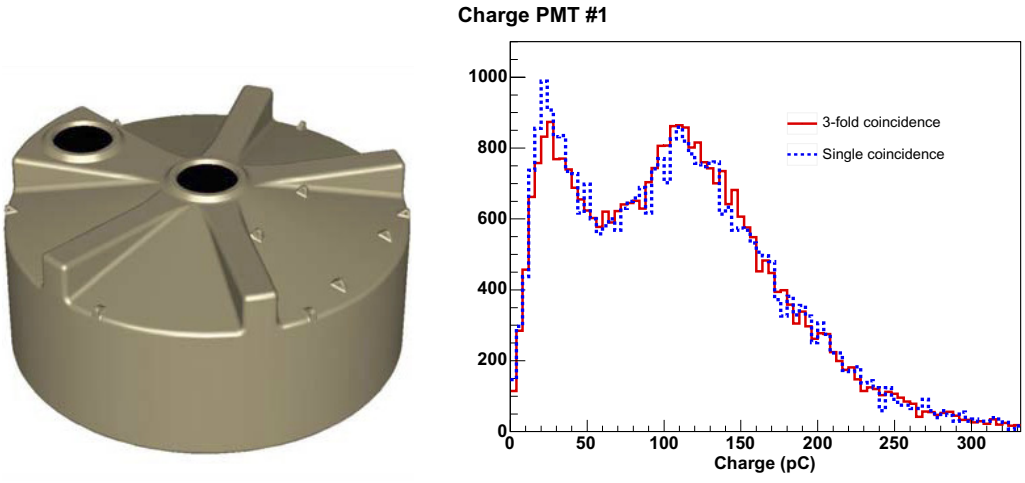

(a) Model tank for Auger North (b) Charge spectrum for single muons

Figure 9. (a) Tanks for Auger North will have only one PMT; the climate in Colorado, USA, requires thermal insulation. (b) Charge spectra for single muons are shown for 3 PMTs in coincidence (solid red line) and for a single PMT: the peak position that defines the energy deposition unit can be determined also with a single PMT.

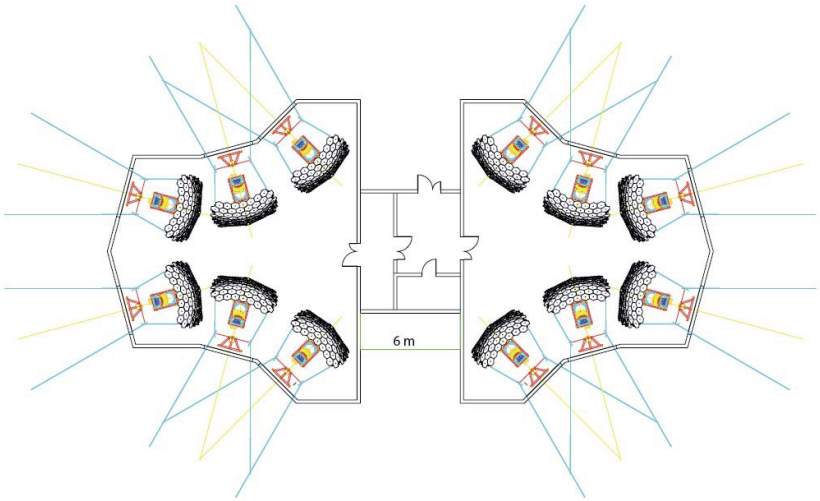

(a) Model FD site

Figure 10. (a) A possible fluorescence telescope site architecture is shown. The field of view is 360° in azimuth and 30° in elevation.

5.2. The FD

The arrangement of telescope buildings across the site is shown in figure 8 and a possible architecture for a 360-degree FD station is shown in figure 10. Behind a robust commercial shutter, a $2.5 \times 2.5\,\mathrm{m}^2$ window made of UV-transmitting filter glass with high absorption in the

visual range reduces background photons. The aperture of the Schmidt optics has a diameter of 2.2 m; an annular-shaped corrector lens with an inner radius of 1.7 m is fitted to reduce spherical aberrations. The transmitted light is collected by a 14 m^2 spherical mirror with 3.4 m radius. The camera in the focal surface of the optical system includes a PMT array of 440 PMTs arranged in 22 rows and 20 columns. The field of view is 1.5° per pixel.

Nearly all electronic boards have been redesigned to improve the performance and to avoid problems with obsolete components. A camera pixel is marked as triggered as long as a running sum exceeds an adjustable threshold value. The time resolution of this first level trigger will be 50 ns. The pixel trigger rate will be measured in intervals of several seconds and automatically adjusts the threshold to limit the rate to about 100 Hz in spite of varying light conditions. A second level trigger will find track segments in the composed camera image, and release a trigger to start the software controlled readout process. A central GPS clock will be used to distribute timing and control signals. An application program running on a separate computer ensures that the sensitive instrument only operates under safe conditions.

5.3. Calibration and atmospheric monitoring

The absolute photometric calibration of the FD telescopes is determined by a drum-shaped light source placed temporarily over a telescope's entrance window. Pulsed UV-light-emitting diodes of different wavelengths inside the drum can be configured to provide a calibrated light flux approximating air shower intensity, distributed uniformly across the entrance aperture and across the angular range of light recorded from air showers. The tracks produced by calibrated vertical nitrogen laser systems located at 3–4 km from each eye will be recorded every night. The stability of the absolute calibration will be monitored by a relative calibration system.

The transmission of fluorescence light in the atmosphere is affected by the aerosol content of the atmosphere that can include haze, dust, smoke, other pollutants and clouds. These conditions can be variable on short timescales and on distance scales much smaller than the size of the array. The northern site will include distant laser facilities (DLF) arranged to span the entire FD aperture (see figure 8). The DLFs generate UV tracks in the fluorescence telescopes similar to high-energy showers. A backscatter light detection and ranging system (LIDAR) will be located near each of the FD sites to locate clouds and to measure local aerosols. Each FD site will also be equipped with cloud cameras. A xenon flash lamp will fire a horizontal, collimated beam of light across the front of an FD to measure the aerosol differential scattering cross-section. The vertical profile of atmospheric depth and air density will be derived from radiosonde data collected twice daily at nearby airports.

5.4. Communications and data acquisition

The entire observatory needs reliable real-time wireless telecommunication for control and data collection across a vast geographical area. The terrain at Auger North is not as flat as that at Auger South and there are no hills on the perimeter. This makes the communication scheme of Auger South, in which each tank transmits to a distant collection point, impractical at Auger North. In the Auger North communications scheme, the data are passed from detector to detector and on to the collection point. The Auger North protocol has been tested in a laboratory setting using 16 radios. In Auger South, the communications system uses the 902–928 MHz band for industrial, scientific and medical (ISM) use, in which an Argentine federal government decree gives Auger priority. For Auger North, ISM bands are less suitable due to the much higher usage

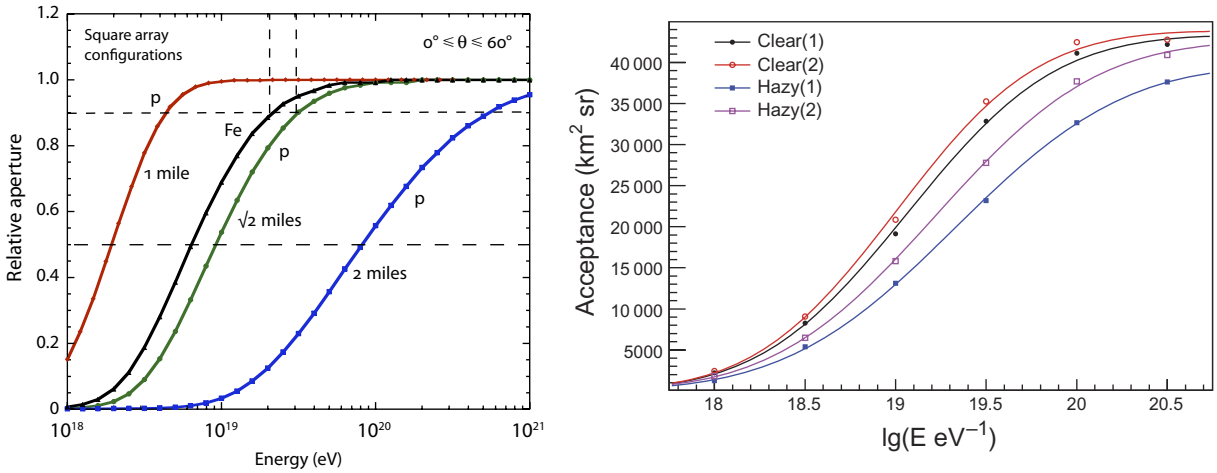

(a) SD trigger efficiency (b) FD acceptance

Figure 11. Detection efficiency and relative aperture of three Auger North SD array candidates. (a) Saturation curves for a square array with a side of 1 mile, $\sqrt{2}$ miles and 2 miles, as indicated. All curves are for proton primaries, except for the case of $\sqrt{2}$ miles where the saturation curve for Fe primaries is also shown, for comparison. (b) Calculated FD acceptance under four atmospheric conditions. Two of them ('clear(1)' and 'clear(2)') correspond to the clear conditions observed during winter and spring. Two models ('hazy(1)' and 'hazy(2)') refer to the somewhat worse conditions during summer.

of wireless devices in the US; therefore, a specific assignment of radio bands for Auger North has been obtained to avoid competition with other users for the radio spectrum. In summer 2008, the radio links between selected positions in the array were tested; calculations based upon digital elevation maps of the area and a single knife edge diffraction model were found to predict accurately the measured path losses.

6. Expected performances

It is important that the trigger efficiency or aperture is well understood as a function of energy, in particular, when the spectral index changes in the energy range concerned. The aperture has been studied using Monte Carlo simulations of the Auger North detector configuration. The simulations were verified using real data from Auger South, in which only sub-sets of SD stations were used such that the spacing resembled the sparser array projected for Auger North. The relative aperture is shown in figure 11 for three SD array spacings that might be implemented in the northern site. The one-mile grid is too expensive to be used on the entire site; the two-mile grid reaches full efficiency only above 1000 EeV. The $\sqrt{2}$-mile grid is a viable compromise in that it becomes fully efficient essentially at the energy where the anisotropy of arrival direction develops. Our estimates show that a 90% efficiency is reached around 20 EeV for Fe primaries and 30 EeV for proton primaries.

The one-mile square array will be fully efficient at a much lower energy, with more than 90% efficiency down to 4 EeV. At these energies the rate of events is correspondingly higher and it is sufficient to cover 10% of the SD area with a denser in-fill array.

Neutrinos may produce a shower close to the SD by interacting deeply in the atmosphere or by skimming the earth crust, both of which occur at very high zenith angles. The sparse northern grid leads to a shift of the neutrino detection efficiency to higher energies. The sensitivity of Auger North to neutrinos will therefore be at the same level as Auger South.

Using a Monte-Carlo simulation and comparing the reconstructed arrival direction with the simulated one, the accuracy in the determination of the arrival direction of the cosmic rays was estimated. For a fixed energy of 50 EeV, the resolutions are 2.2°, 1.2° and better than 1° for zenith angles of 25°, 45° and 60°, respectively.

The procedure to reconstruct the cosmic ray energies has been described in [9]. Essentially, the lateral density function (LDF) of the SD signals as a function of the distance from the shower core is fitted; the LDF value at a certain core distance is a good energy estimator of the shower, which then has to be corrected for the shower attenuation in the atmosphere at various zenith angles. The optimal distance depends mainly on the array spacing; for Auger South, we have adopted 1000 m and the energy estimator is called S1000. The absolute energy scale is then set by the calorimetric FD measurement. We found that S1000 should be replaced by S1500 (LDF at 1500 m) to achieve an energy resolution of Auger North similar to that of Auger South. With the same optimization of the reconstruction procedure, the expected core position accuracy is 130 m.

Since the basic design of the FD telescopes is similar for the Northern and Southern Observatories, we can employ the well-tuned detector simulation package currently used for analysis of the Southern site data to evaluate the expected performance of the FD layout described above. The simulations use proton showers generated with the `CONEX` program package [30]. The emission of fluorescence and Cherenkov light is calculated from the longitudinal energy deposit and electron profiles, and the generated photons are propagated towards the telescopes where they are ray-traced through the optics, digitized and sent through the four trigger algorithms currently used in the South [31].

The efficiencies for triggering the FD and for actually reconstructing a high-quality track as a function of distance to the telescopes determine the area that can be covered with one telescope. We used the *US Standard Atmosphere* for the molecular density profiles and studied four different aerosol contaminations that correspond to the clear conditions observed during winter and spring and to the somewhat worse conditions during summer. The results have led us to use 40 km effective viewing distance in the layout for the northern FD. The fraction of stereo or multiple observations of the same shower will be quite small. The FD acceptance as a function of energy for showers that fulfil basic quality selection criteria can be seen in figure 11. It is calculated for zenith angles up to 70° since longitudinal shower profiles can be reliably reconstructed even for inclined showers. The acceptance for the standard SD zenith angle range ($\theta < 60°$) is about 20% smaller. At 100 EeV, the expected acceptance is 42 000 km^2 sr for clear atmospheric conditions and 35 000 km^2 sr in the summer months. Since more data are collected during winter, when the nights are longer, we expect the average aperture at ultra-high energies to be at around 40 000 km^2 sr corresponding to an effective site coverage of 70%.

7. Organization

The Auger Collaboration is comprised of scientists from 18 countries: Argentina, Australia, Bolivia, Brazil, Croatia, Czech Republic, France, Germany, Italy, Mexico, Netherlands, Poland, Portugal, Slovenia, Spain, United Kingdom, United States and Vietnam. This organization will

be the first consortium in astroparticle physics to build and operate two very large sites as a single instrument, the Pierre Auger Observatory.

The estimated total construction cost of Auger North is \$127M using the well-established Work Breakdown Structure (WBS) accounting scheme. Fund-raising efforts are ongoing in all member countries. We plan to construct the Northern Auger site from 2011 until 2016. The operating costs for Auger North are based on experience in operating the southern site, factoring in the greater size of Auger North and taking differences in the costs for goods and services at the two sites into account. The estimated total is \$5.5M per year, which corresponds to a little less than 5% of the projected capital cost.

8. Other projects: Telescope Array (TA), JEM-EUSO

The AGASA detector was previously the largest ground array, covering 110 km^2 in Japan; it reached a final exposure of 1630 km^2 sr yr after 12 years of operation. The FDs Fly's Eye and its successor HiRes in Utah/USA finally reached close to 10 000 km^2 sr yr.

The mission of the ongoing TA project and its low-energy extension TALE are the study of the transition region of galactic to extragalactic cosmic rays and the resolution of the discrepancies between AGASA and HiRes data [32]. TA is a hybrid system of ground detectors and fluorescence telescopes located in Millard County, Utah. The ground array consists of 507 detector stations, each built up of two layers of scintillators of 3 m^2 area. The detector positions form a rectangular grid of 1.2 km spacing covering a total area of about 700 km^2. Three fluorescence stations are deployed at the apices of an equilateral triangle of 30 km side length. Regular data taking started in March 2008. The aperture of TA at 100 EeV is 1200 km^2 sr for the ground detector complemented with the FD acceptance of 470 km^2 sr (mono) and 290 km^2 sr (stereo).

The Extreme Universe Space Observatory (JEM-EUSO) on the Japanese Experiment Module on the International Space Station (ISS) aims to reach much larger apertures by observing the dark part of the atmosphere from space. The basic idea is to observe the fluorescence light of air showers from space as a series of digital images, see Takahashi *et al*, this NJP issue [33]. JEM-EUSO is targeting a launch in 2014 in the framework of a second phase of the JEM/EF utilization. The main component of JEM-EUSO is an UV telescope mounted on the ISS. The field of view of 60° from a 430 km orbiting altitude corresponds to the observation of a circular area of 250 km radius. Assuming 10% duty cycle, the effective geometric aperture would thus be 6×10^4 km^2 sr. The expected resolutions for shower direction (2.5°) and $X_{\mathrm{max}}(150\,\mathrm{g\,cm}^{-2})$ are inferior to the proven performance of ground arrays; however, the project may open a novel technology and pave the way to larger exposures.

9. Summary

We have shown that there are extremely interesting challenges in the particle physics and astrophysics of UHE cosmic rays. The technologies are readily available to address these issues. Figure 12 shows the exposures of contemporary cosmic ray observatories as a function of time. The dramatic increase over previously achieved exposures by the Auger South and Auger North observatories is evident and translates directly into statistical power and discovery potential for the most energetic cosmic particles. Eventually, the information from all messenger particles like photons, nuclei and neutrinos will have to be combined.

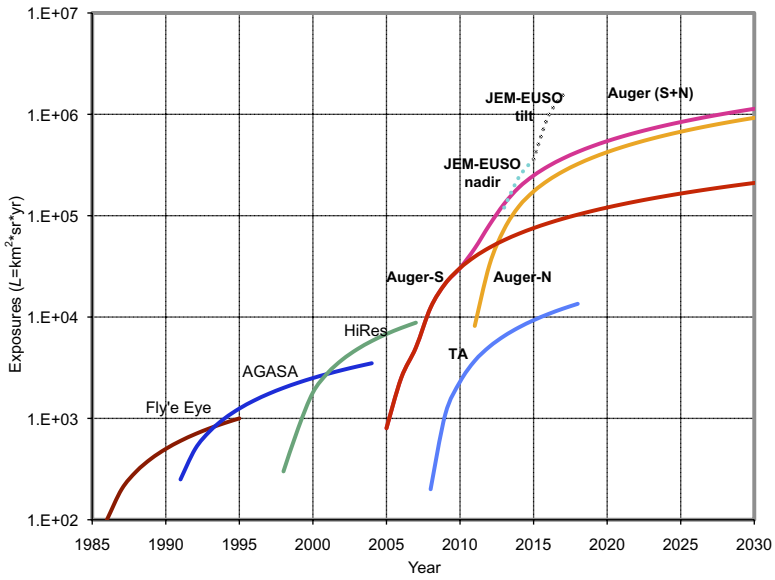

(a) Exposures as a function of time

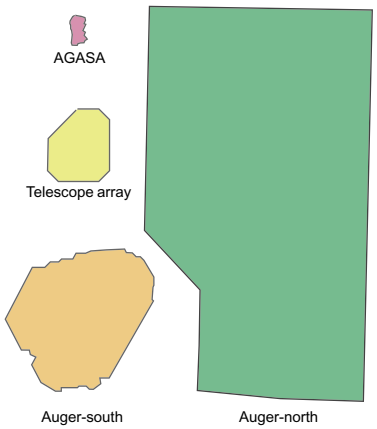

(b) Footprint of ground-based cosmic ray observatories (to scale)

Figure 12. (a) Exposures of cosmic ray observatories as a function of time. The JEM-EUSO project is a planned space-born instrument on the ISS, whereas the other installations are ground-based; see text for further details. (b) The relative collection areas of the AGASA, TA, Auger South and Auger North arrays are shown.

Acknowledgments

The successful installation and commissioning of the Pierre Auger Observatory would not have been possible without the strong commitment and effort from the technical and administrative staff in Malargüe.

The effort expended on the design and layout of the northern site of the Pierre Auger Observatory is the work of many colleagues on all continents. Their contributions—summarized in this paper and to appear in more detail in the *Auger North Design Report* (to be published)—are gratefully acknowledged.

We are very grateful to the following agencies and organizations for financial support: Comisión Nacional de Energía Atómica, Fundación Antorchas, Gobierno De La Provincia de Mendoza, Municipalidad de Malargüe, NDM Holdings and Valle Las Leñas, in gratitude for their continuing cooperation over land access, Argentina; the Australian Research Council; Conselho Nacional de Desenvolvimento Científico e Tecnológico (CNPq), Financiadora de Estudos e Projetos (FINEP), Fundação de Amparo à Pesquisa do Estado de Rio de Janeiro (FAPERJ), Fundação de Amparo à Pesquisa do Estado de São Paulo (FAPESP), Ministério de Ciência e Tecnologia (MCT), Brazil; AVCR AV0Z10100502 and AV0Z10100522, GAAV KJB300100801 and KJB100100904, MSMT-CR LA08016, LC527, 1M06002, and MSM0021620859, Czech Republic; Centre de Calcul

IN2P3/CNRS, Centre National de la Recherche Scientifique (CNRS), Conseil Régional Ile-de-France, Département Physique Nucléaire et Corpusculaire (PNC-IN2P3/CNRS), Département Sciences de l'Univers (SDU-INSU/CNRS), France; Bundesministerium für Bildung und Forschung (BMBF), Deutsche Forschungsgemeinschaft (DFG), Finanzministerium Baden-Württemberg, Helmholtz-Gemeinschaft Deutscher Forschungszentren (HGF), Ministerium für Wissenschaft und Forschung, Nordrhein-Westfalen, Ministerium für Wissenschaft, Forschung und Kunst, Baden-Württemberg, Germany; Istituto Nazionale di Fisica Nucleare (INFN), Ministero dell'Istruzione, dell'Universitàe della Ricerca (MIUR), Italy; Consejo Nacional de Ciencia y Tecnología (CONACYT), Mexico; Ministerie van Onderwijs, Cultuur en Wetenschap, Nederlandse Organisatie voor Wetenschappelijk Onderzoek (NWO), Stichting voor Fundamenteel Onderzoek der Materie (FOM), Netherlands; Ministry of Science and Higher Education, Grant Nos. 1 P03 D 014 30, N202 090 31/0623, and PAP/218/2006, Poland; Fundação para a Ciência e a Tecnologia, Portugal; Ministry for Higher Education, Science, and Technology, Slovenian Research Agency, Slovenia; Comunidad de Madrid, Consejería de Educación de la Comunidad de Castilla La Mancha, FEDER funds, Ministerio de Ciencia e Innovación, Xunta de Galicia, Spain; Science and Technology Facilities Council, United Kingdom; Department of Energy, Contract No. DE-AC02-07CH11359, National Science Foundation, Grant No. 0450696, The Grainger Foundation USA; ALFA-EC/HELEN, European Union 6th Framework Program, Grant No. MEIF-CT-2005-025057, European Union 7th Framework Program, Grant No. PIEF-GA-2008-220240, and UNESCO.

References

[1] Hess V 1912 *Phys. Z.* **13** 1084
[2] Auger P *et al* 1938 *Comptes Rendue* **206** 1721
[3] Kulikov G and Khristiansen G 1958 *J. Exp. Theor. Phys.* **35** 635
[4] Linsley J 1963 *Phys. Rev. Lett.* **10** 146
[5] Greisen K 1966 *Phys. Rev. Lett.* **16** 748
Zatsepin G T and Kuzmin V A 1966 *Pisma Zh. Eksp. Teor. Fiz.* **4** 114
[6] Nagano M and Watson A A 2000 *Rev. Mod. Phys.* **72** 689
[7] Antoni T *et al* 2002 *Astropart. Phys.* **16** 373
[8] Abraham J *et al* 2007 *Science* **318** 939
Abraham J *et al* 2008 *Astropart. Phys.* **29** 188
[9] Abraham J *et al* 2008 *Phys. Rev. Lett.* **101** 061101
[10] Abbasi R *et al* 2008 *Phys. Rev. Lett.* **100** 101101
[11] Blümer J, Engel R and Hoerandel J 2009 *Prog. Part. Nucl. Phys.* **63** 293
[12] Olinto A V *et al* 2008 White paper on ultra-high energy cosmic rays (arXiv:0805.4779)
[13] Allard D *et al* 2008 *J. Cosmol. Astropart. Phys.* JCAP05(2008)033
[14] Abraham J *et al* 2004 *Nucl. Instrum. Methods* A **523** 50
[15] Allekotte I *et al* 2008 *Nucl. Instrum. Methods* A **586** 409
[16] Abraham J *et al* 2009 *Nucl. Instrum. Methods* A submitted arXiv:0907.4282
[17] Sommers P and Westerhoff S 2009 *New J. Phys.* **11** 055004
[18] The Pierre Auger Collaboration 2009 Calibration and monitoring of the Pierre Auger Observatory. Contribution to the *31st Int. Cosmic Ray Conf. (Lodz, Poland, July 2009)* (*Preprint* arXiv:0906.2358v1 [astro-ph.IM])
[19] The Pierre Auger Collaboration 2009 The cosmic ray energy spectrum and related measurements with the Pierre Auger Observatory. Contribution to the *31st Int. Cosmic Ray Conf. (Lodz, Poland, July 2009)* (*Preprint* arXiv:0906.2189v2 [astro-ph.HE])

[20] The Pierre Auger Collaboration 2009 Studies of cosmic ray composition and air shower structure with the Pierre Auger Observatory. Contribution to the *31st Int. Cosmic Ray Conf. (Lodz, Poland, July 2009)* (*Preprint* arXiv:0906.2319v1 [astro-ph.CO])
[21] Ulrich R, Blümer J, Engel R, Schüssler F and Unger M 2009 *New J. Phys.* **11** 065018
[22] The Pierre Auger Collaboration 2009 Astrophysical sources of cosmic rays and related measurements with the Pierre Auger Observatory. Contribution to the *31st Int. Cosmic Ray Conf. (Lodz, Poland, July 2009)* (*Preprint* arXiv:0906.2347v2 [astro-ph.HE])
[23] Abraham J *et al* 2007 *Astropart. Phys.* **27** 244
[24] Lee S 1998 *Phys. Rev.* D **58** 043004
[25] Abraham J *et al* 2009 *Astropart. Phys.* **31** 399 (*Preprint* arXiv:0903.1127v2)
[26] Abraham J *et al* 2009 *Phys. Rev.* D **79** 102001 (*Preprint* arXiv:0903.3385)
[27] Ackermann M *et al* (IceCube) 2008 *Astrophys. J.* **675** 1014
Kravchenko I *et al* (RICE) 2006 *Phys. Rev.* D **73** 082002
Gorham P W *et al* (ANITA) 2008 arXiv:0812.2715v1
Abbasi R U *et al* (HiRes) 2008 *Astrophys. J.* **684** 790
Martens K 2007 arXiv:0707.4417
[28] Cooper-Sarkar A and Sarkar S 2008 *J. High Energy Phys.* JHEP01(2008)075
[29] The Pierre Auger Collaboration 2009 Operations and future plans for the Pierre Auger Observatory. Contribution to the *31st Int. Cosmic Ray Conf. (Lodz, Poland, July 2009)* (*Preprint* arXiv:0906.2354v2 [astro-ph.IM])
[30] Bergmann T *et al* 2007 *Astropart. Phys.* **26** 420
[31] Prado L *et al* 2005 *Nucl. Instrum. Methods* A **545** 632
[32] Nonaka T *et al* 2009 *Nucl. Phys. B* **190** 26
[33] Takahashi Y *et al* 2009 *New J. Phys.* **11** 065009